Electropolymerization of *O*-Phenylenediamine on Pt-Electrode from Aqueous Acidic Solution: Kinetic, Mechanism, Electrochemical Studies and Characterization of the Polymer Obtained

S. M. Sayyah, M. M. El-Deeb, S. M. Kamal, R. E. Azooz

Chemistry Department, Polymer Research Laboratory, Beni-Suef University, 62514 Beni-Suef, Egypt

Received 14 June 2008; accepted 8 October 2008
DOI 10.1002/app.29802
Published online 12 March 2009 in Wiley InterScience (www.interscience.wiley.com).

ABSTRACT: Electropolymerization of *O*-phenylenediamine (*o*-PD) on Pt-electrode from a deoxygenated aqueous acid medium was carried out using cyclic voltammetry technique. The kinetic parameters were calculated by means of electrochemical data. The experimentally obtained kinetic equation was $R_{P,E} = k_E$ [monomer]$^{1.19}$ [acid]$^{1.23}$ [electrolyte]$^{0.87}$ from the value of the anodic current density using cyclic voltammetry technique. The apparent activation energy (E_a) is found to be 28.34 kJ mol^{-1}. The polymer films obtained have been characterized by X-ray diffraction, elemental analysis, scanning electron microscopy, ^{1}H-NMR, ^{13}C-NMR, UV-visible, and IR spectroscopy. The mechanism of the electrochemical polymerization reaction has been discussed. TGA is used to confirm the proposed structure and determination of the number of water molecules in the polymeric chain unit. © 2009 Wiley Periodicals, Inc. J Appl Polym Sci 112: 3695–3706, 2009

Key words: electropolymerization; kinetic; cyclic voltammetry; thermal analysis; mechanism

INTRODUCTION

Electropolymerization of conducting polymers on electrode surfaces is one of the targets of the research work area in electrochemistry. The great deal of attention in this area is due to the large number of potential applications of conducting polymer itself as well as the modified electrode surfaces; in batteries, electrochromic devices, microelectronic devices, optoelectronic, display devices, chemically modified electrodes, sensors, electrochemical chromatography, metallization, and as corrosion inhibitors to protect semiconductors and metals.[1–28]

The oxidative polymerization of aromatic diamines and the obtained polymers have been extensively investigated. The polymers exhibit a number of advantages including the choice of monomer, diversity, and facility of polymerization via oxidation of one or both amino groups, variety of macromolecular structure, variability of electroconductivity, multifunctionality due to one free amino group per repetitive unit on the polymers and potentially wide applicability. The polymerization mechanism and properties of the polymers have not been definitely reported.

Most of the aromatic diamines polymers have been prepared by electrochemical polymerization, but only a small number of polymers were obtained through chemically oxidative polymerization. Investigations on enzyme- and photo-catalyzed oxidative polymerizations are very rare.

Poly(*ortho*-phenylenediamine) P(*o*-PD) has many attractive properties. P(*o*-PD) can be prepared electrochemically in acid, neutral, and alkaline solutions and is very stable in both aqueous solutions and air.[29–38] The ease of dissolution of P(*o*-PD) in organic solvents, such as dimethylsulfoxide (DMSO), dimethylformamide (DMF), and etc., makes it one of the so-called soluble electroactive polymers and thus provides more flexibility in the studies of its structures.[36,37] Different types of working electrodes were used including Pt, Au, GC, ITO, PB/ITO, and graphite.

To the best of the our knowledge, the kinetic studies of electrochemical preparation of P(*o*-PD) are not investigated in the literature but, in case of the structure of P(*o*-PD), there are many trails in the literature.[34–38]

Sayyah et al. studied the kinetic of the electropolymerization process of different substituted aromatic

Correspondence to: S. M. Sayyah (smsayyah@hotmail.com).

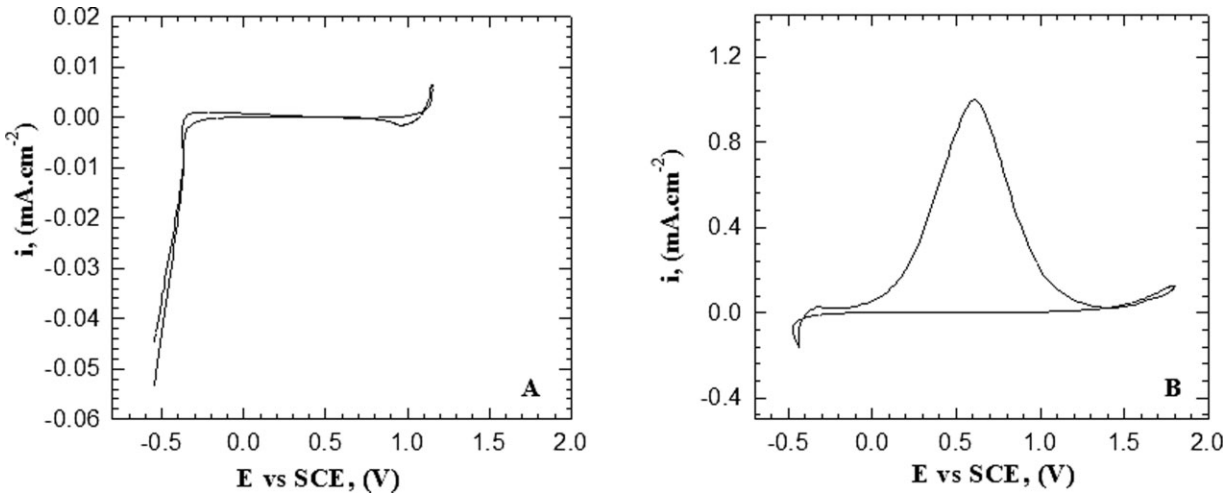

Figure 1 Cyclic voltammogram of Pt-electrode from solution containing 0.5*M* HCl and 0.1*M* Na_2SO_4 at 290 K with scan rate of 25 m Vs^{-1} in (A) absence of monomer, (B) 0.08*M* monomer.

amines. The kinetic equations were calculated from *ex situ* microgravimetric data[39–45] and from both the microgravimetric and electrochemical data.[46,47]

In this study, we intend to investigate the electrodeposition of P(*o*-PD) on Pt electrode from aqueous HCl solution using cyclic voltammetry technique. The kinetics, optimum conditions, and mechanism of the electrochemical polymerization will be discussed using electrochemical data. Also, the characterization of the obtained polymer film should be done by ^{1}H-NMR, IR, elemental analysis, TGA, SEM, and X-ray diffraction.

EXPERIMENTAL

Materials

O-phenylenediamine (Merck-Darmstadt, Germany) was purified by twice recrystallization from water as described else where,[32,36,42] hydrochloric acid solution (Riedel-de Haën, Germany) and Dimethylformamide were provided by El-Naser pharmaceutical Chemical Company (Egypt), anhydrous sodium sulfate was provided by Merck (Darmstadt, Germany). All solutions were prepared under nitrogen atmosphere in freshly double-distilled water.

Cell and electrodes

A standard three-electrode cell was used in the cyclic voltammetry measurements with a saturated calomel electrode (SCE) as the standard reference electrode. The auxiliary electrode was a platinum wire. The dimensions of the platinum working electrode were 1 × 0.5 × 0.05 cm. Before each run, the working electrode was cleaned and washed with distilled water, rinsed with ethanol, and then dried.

The electrochemical experiments were performed using the Potentiostat/Galvanostat Wenking PGS 95. The I-E curves were recorded by computer software from the same company (Model ECT).

IR, elemental analysis, ^{1}H-NMR, ^{13}C-NMR, UV-Vis, and TGA

IR measurements were carried out using Shimadzu Ftir-340 Jasco spectrophotometer.

Elemental analysis was carried out in the microanalytical center at Cairo University by oxygen flask combustion and dosimat E415 titrator (Metrohm).

^{1}H-NMR and ^{13}C-NMR measurements were carried out using a Varian EM 360 L, 60-MHz NMR spectrometer. NMR and ^{13}C-NMR signals of the

Scheme 1 Different structures of the oxidized form of P(*o*-PD).

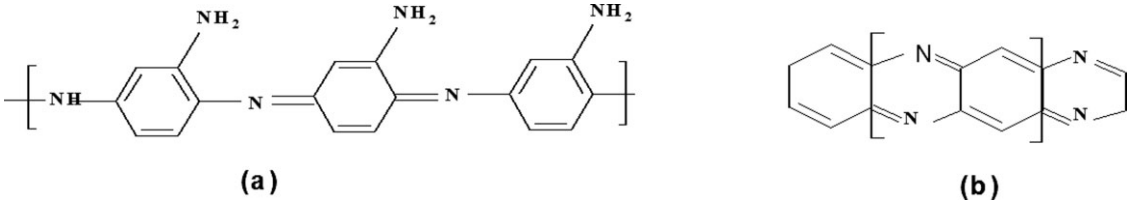

Scheme 2 different structures of P(*o*-PD).

electropolymerized samples were recorded in dimethylsulphoxide using tetramethylsilane as internal reference.

The ultraviolet-visible absorption spectra of the prepared polymer samples were measured using Shimadzu UV spectrophotometer (M160 PC) at room temperature in the range 200–900 nm using dimethylformamide as a solvent and reference.

TGA of the obtained polymer was performed using a Shimadzu DT-30 thermal analyzer (Shimadzu, Kyoto, Japan). The weight loss was measured from ambient temperature up to 600°C, at the rate of 20°C min^{-1} to determine the degradation rate of the polymer

Scanning electron microscopy and X-ray diffraction

Scanning electron microscopic analysis was carried out using a JXA-840A Electron Probe Microanalyzer (JEOL, Tokyo, Japan). The X-ray diffractometer (Philips 1976 Model 1390, Netherlands) was operated

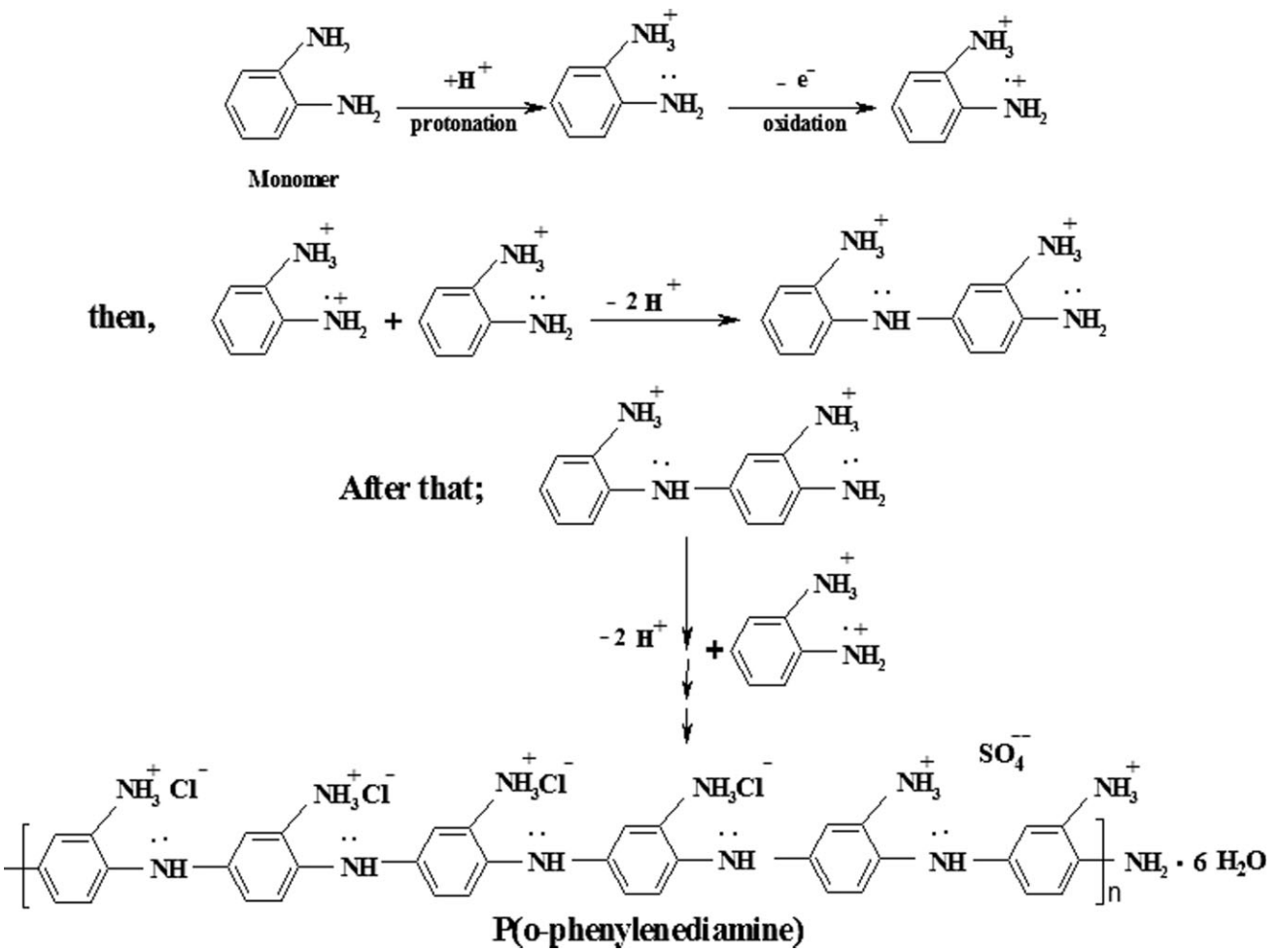

Scheme 3 The propagation and formation of P(*o*-PD).

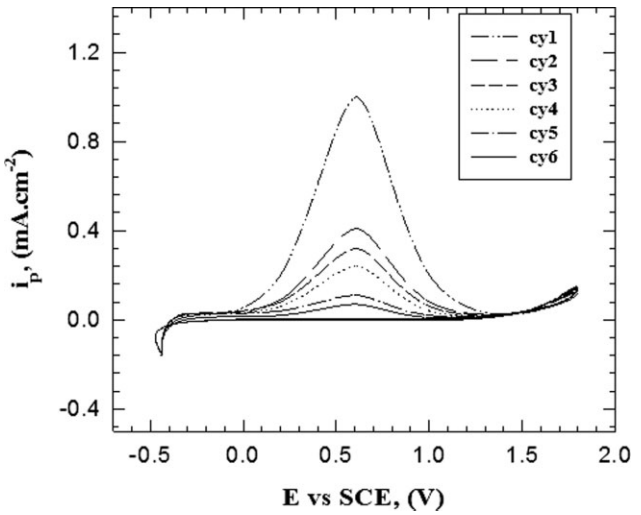

Figure 2 Repetitive cycling of electropolymerization of *o*-phenylene diamine from solution containing 0.08*M* monomer, 0.5*M* HCl, and 0.1*M* Na_2SO_4 at 290 K with scan rate of 25 m Vs^{-1}.

under the following conditions that were kept constant for all the analysis processes:

X-ray tube: Cu Scan speed: 8° min^{-1}
Current: 30 mA Voltage: 40 kV
Preset time: 10 s.

RESULT AND DISCUTION

Electropolymerization of *o*-phenylenediamine (*o*-PD) and mechanism

Electropolymerization of *o*-phenylenediamine on platinum electrode from the deoxygenated aqueous solution containing 0.5*M* HCl, 0.08*M* monomer, and 0.1*M* Na_2SO_4 at 290 K, in the absence and presence of monomer, was studied by cyclic voltammetry at potential between −440 and +1790 mV (versus SCE) with scan rate of 25 m Vs^{-1}. The obtained voltammogram is represented in Figure 1(A,B), respectively. In the absence of monomer, no peaks are observed where in the presence of monomer, a well-adhering P(*o*-PD) film is electrodeposited on the electrode surface. The voltammogram exhibits only one irreversible distinct anodic peak, at +609 mV (versus SCE), in the anodic excursion.

For the structure of the obtained oxidized form of P(*o*-PD), two different opinions have been suggested. Oyama and coworkers[34] presumed monohydrophenazine rings (Structure "a" represented in Scheme 1, for the polymeric backbone. In contrast, Wu et al.[38] proposed more oxidized phenazine rings (Structure "b" represented in Scheme 1 on the basis of an *in situ* resonance Raman spectroscopic study.

In the literature, two different structure of P(*o*-PD) (cf. Scheme 2) (a) a "ladder" like structure by Oyama and coworkers,[34] and (b) a 1,4-substituted benzenoid-quinoid "open" structure by Yano.[37]

One of the amino groups of *o*-phenylenediamine monomer in acidic solution must be protonated.[37] The positively charged ammonium group without a lone electron pair probably hinders the formation of the phenazine ring during electropolymerization and then has the meta orientation effect. Therefore, the head-to-tail coupling must be favorable for the *o*-phenylenediamine polymerization, leading to the formation of poly(aminoaniline).

The oxidation peak corresponds to the oxidation of *o*-phenylenediamine monomer and removal of an electron from the nitrogen atom of the amino group to form a radical cation, which interacts with another monomer molecule to form a dimer radical cation, trimer radical cation, and so on; finally, we obtain 1,4-substituted benzenoid "open" structure as shown in Scheme 3.

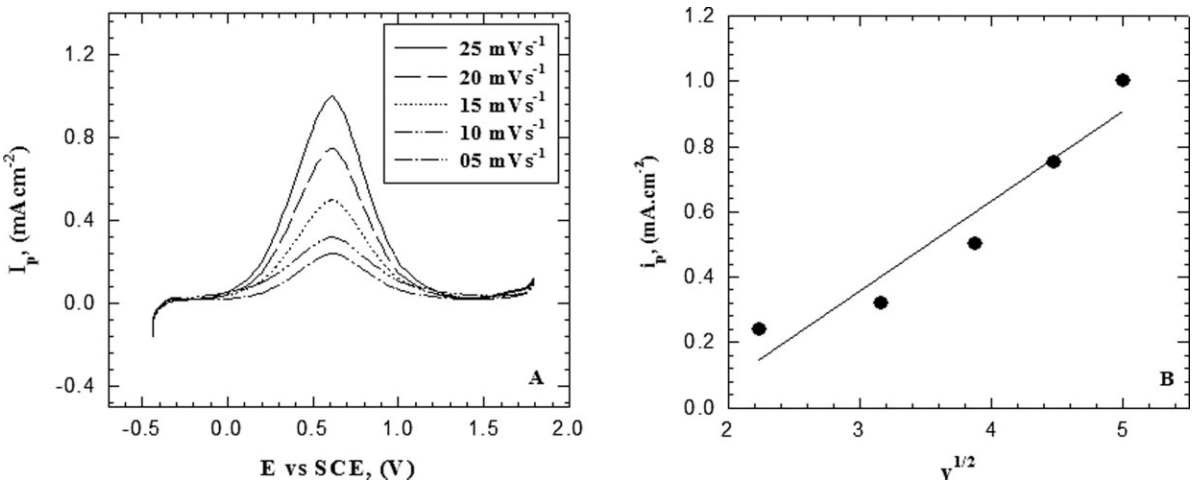

Figure 3 (A) Effect of Scan rate on the of electropolymerization of *o*-phenylenediamine from solution containing 0.08*M* monomer, 0.5*M* HCl, and 0.1*M* Na_2SO_4 at 290 K. (B) Relation between i_p versus $v^{1/2}$.

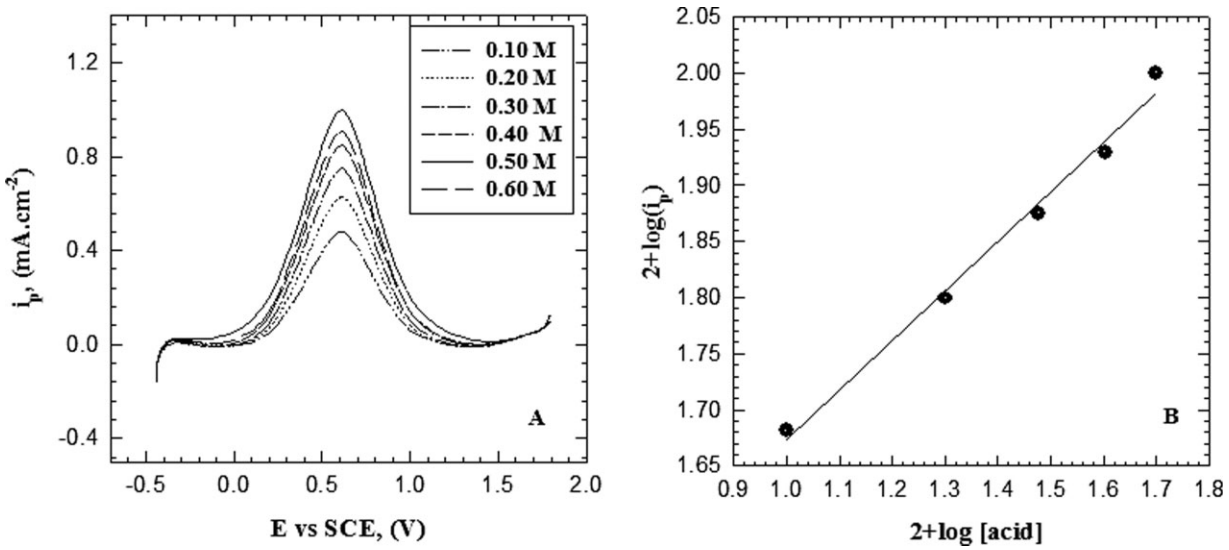

Figure 4 (A) Potentiodynamic polarization curves for the effect of HCl concentration on the electropolymerization of *o*-phenylenediamine from solution containing 0.08*M* monomer and 0.1*M* Na_2SO_4 at 290 K with scan rate of 25 m Vs^{-1}. (B) Double logarithmic plot of the anodic current densities versus HCl concentrations.

Figure 2 shows the effect of repetitive cycling on the formation of the polymer film from the deoxygenated aqueous solution containing 0.5*M* HCl, 0.08*M* monomer, and 0.1*M* Na_2SO_4 at 290 K. The data reveal that, the peak current densities (i_p) decrease with repetitive cycling. The potential position of the redox peak does not shift with increasing number of cycles, indicating that the redox reaction is independent on the polymer thickness.

Figure 3(A) illustrates the influence of the scan rate (5–25 m Vs^{-1}) on the potentiodynamic anodic polarization curves for *o*-phenylenediamine from the deoxygenated aqueous solution containing 0.5*M* HCl, 0.08*M* monomer, and 0.1*M* Na_2SO_4 at 290 K on platinum electrode. It is obvious that the anodic peak current densities (i_p) increase with the increasing of the scan rate.

Figure 3(B) shows the linear dependency of i_p versus $v^{1/2}$. This linear relation suggests that the electropolymerization of *o*-phenylenediamine may be described by a partially diffusion-controlled process (diffusion of reacting species to the polymer film/solution interface).

Kinetic studies

The electropolymerization kinetics were evaluated using deoxygenated aqueous solution containing monomer in the concentration range between 0.01 and 0.08*M*, hydrochloric acid concentration in the

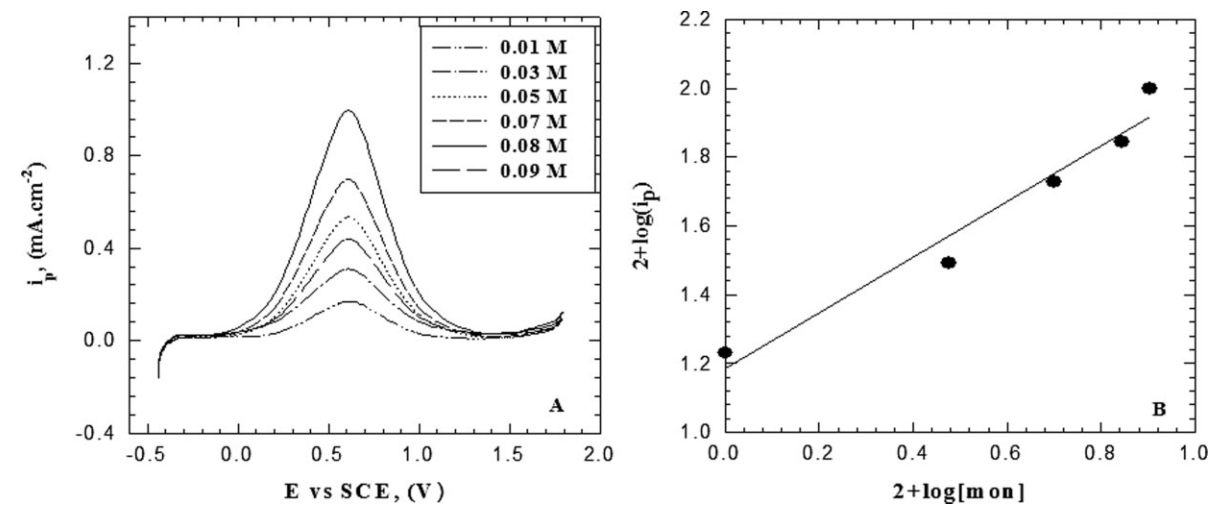

Figure 5 (A) Potentiodynamic polarization curves for the effect of monomer concentration on the electropolymerization of *o*-phenylenediamine from solution containing 0.5*M* HCl and 0.1*M* Na_2SO_4 at 290 K with scan rate of 25 m Vs^{-1}. (B) Double logarithmic plot of the anodic current densities versus monomer concentrations.

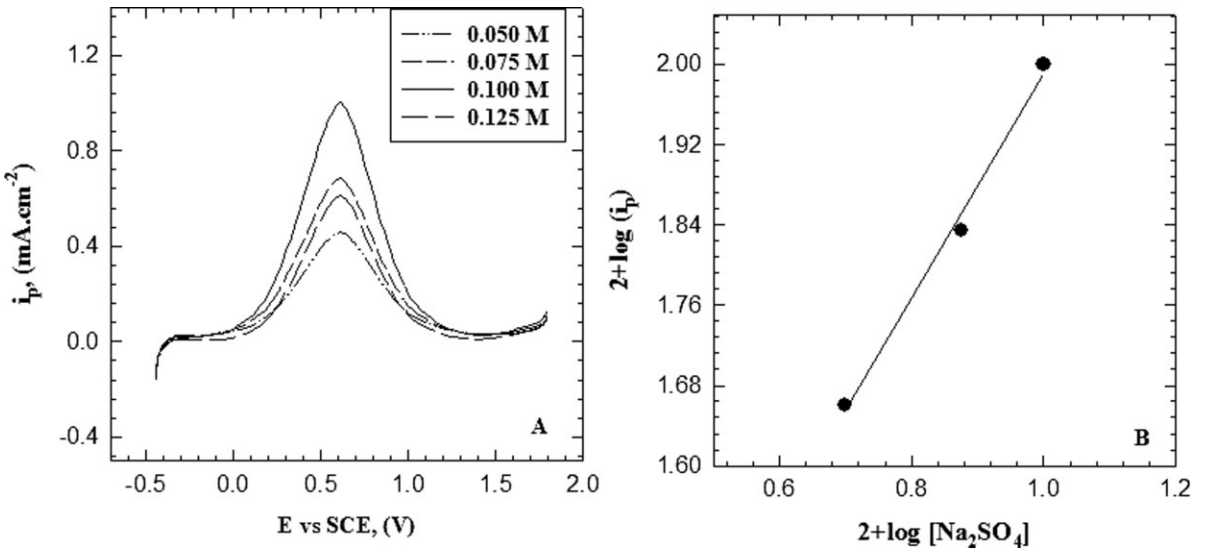

Figure 6 (A) Potentiodynamic polarization curves for the effect of electrolyte concentration on the electropolymerization of *o*-phenylenediamine from solution containing 0.5*M* HCl and 0.08*M* monomer at 290 K with scan rate of 25 m Vs^{-1}. (B) Double logarithmic plot of the anodic current densities versus electrolyte concentrations.

range between 0.1 and 0.5*M*, and Na_2SO_4 in the concentration range between 0.05 and 0.10*M* at 290 K. The kinetic equation was calculated by means of electrochemical study from the values of the anodic current densities.[46,47]

The value of the anodic current density (i_p) is proportional to the electropolymerization rate ($R_{P,E}$) at a given concentration of the monomer, acid, and electrolyte; then, we can replace the electropolymerization rate by the anodic current density.[46,47]

The effect of HCl concentration, monomer concentration, supporting electrolyte concentration, and temperature on the cyclic voltammetric characteristics for the polymer film formation on Platinum electrode surface was investigated.

Effect of HCl concentration

Figure 4(A) represents the influence of HCl concentration in the range between 0.1 and 0.6*M* on the cyclic voltammogram using scan rate of 25 m Vs^{-1}. The voltammogram shows that, the anodic peak current densities (i_p) increase with the increasing of the HCl concentration up to 0.5*M* and then starts to decrease with further increase of HCl concentration as a result of degradation and solubility of the

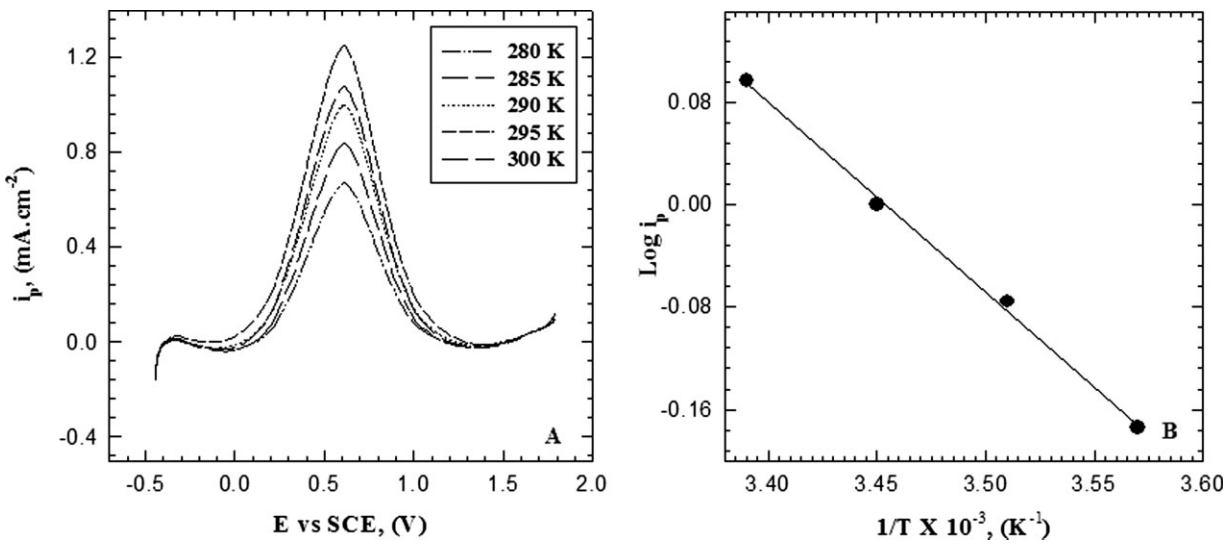

Figure 7 (A) Potentiodynamic polarization curves for the effect of temperature on the electropolymerization of *o*-phenylenediamine from solution containing 0.5*M* HCl, 0.08*M* monomer and 0.1*M* Na_2SO_4 with scan rate of 25 m Vs^{-1}. (B) Arrhenius plot of the of electropolymerization of *o*-phenylenediamine.

TABLE I
Elemental Analysis of the Prepared P(*o*-PD)

Element (%)									
C		H		N		Cl		S	
Calc.	Found	Calc.	Found	Calc.	Found	Calc.	Found	Calc.	Found
43.68	42.17	5.56	5.78	16.98	15.26	14.36	13.81	3.23	3.02

formed polymer film. A double logarithmic plot of the current density related to oxidation peak against HCl concentrations in the range between 0.1 and 0.5*M* is graphically represented in Figure 4(B). A straight line with slope of 1.23 was obtained. Therefore, the reaction order with respect to HCl concentration is a first-order reaction.

Effect of monomer concentration

Figure 5(A) represents the influence of monomer concentration in the range between 0.01 and 0.09*M* on the cyclic voltammogram using scan rate of 25 m Vs^{-1}. The voltammogram shows that, the anodic peak current densities (i_p) increase with the increasing of the monomer concentration up to 0.08*M* and then starts to decrease with further increase of monomer concentration. A double logarithmic plot of the current density related to oxidation peak against monomer concentrations in the range between 0.01 and 0.08*M* is graphically represented in Figure 5(B). A straight line with slope of 1.19 was obtained. Therefore, the reaction order with respect to monomer concentration is a first-order reaction.

Effect of electrolyte concentration

Figure 6(A) shows the effect of Na_2SO_4 concentration, as a dopant (which is confirmed by IR study), in the range between 0.05 and 0.125*M* on the cyclic voltammogram using scan rate of 25 m Vs^{-1}. The anodic peak current densities (i_p) increase with the increasing of the Na_2SO_4 concentration up to 0.1*M* and then starts to decrease with further increase of Na_2SO_4 concentration. A double logarithmic plot of the current density related to oxidation peak against Na_2SO_4 concentrations in the range between 0.05 and 0.1*M* is graphically represented in Figure 6(B). A straight line with slope of 0.87 was obtained.

Depending upon the above results, the kinetic rate law obtained from this method can be written as follows:

$$R_{P,E} = k_E[\text{monomer}]^{1.19}[\text{acid}]^{1.23}[\text{electrolyte}]^{0.87}$$

Where, $R_{P,E}$ is the electropolymerization rate and k_E is the kinetic rate constant.

Effect of temperature

The potentiodynamic polarization curves as a function of the solution temperature in the range between 280 and 300 K under the same experimental conditions as mentioned above were illustrated in Figure 7(A). From the figure, it is clear that, an increase of temperature up to 295 K results in a progressive increase of the charge included in the anodic peak. The plot of the log (i_p) versus $1/T$ is represented in Figure 7(B), a straight line is obtained with a slope equal to −1.48 and then the apparent activation energy was calculated using Arrhenius equation and it is found to be 28.34 kJ mol^{-1}.

Elemental and spectroscopic analysis

Elemental analytical data are given in Table I, which are in a good agreement with those calculated from the suggested structure given in Scheme 3.

The presence of six water molecules for each repeated unit is confirmed by thermogravimetric analysis. The TGA steps of the prepared P(*o*-PD) are shown in Figure 8 and summarized in Scheme 4. From the scheme, it is clear that, there are five stages during thermolysis of the polymer sample.

First stage

It includes the loss of ($1H_2O + SO_3$) molecules in the temperature rang between 25 and 131.6°C. The weight loss for this step was found to be (9.68%)

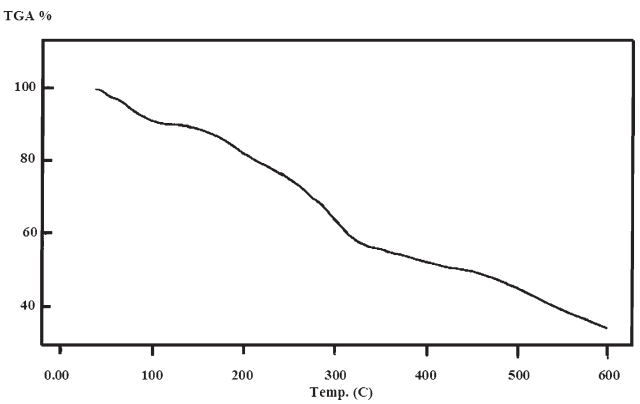

Figure 8 TGA of prepared poly(*o*-phenylenediamine) at optimum conditions.

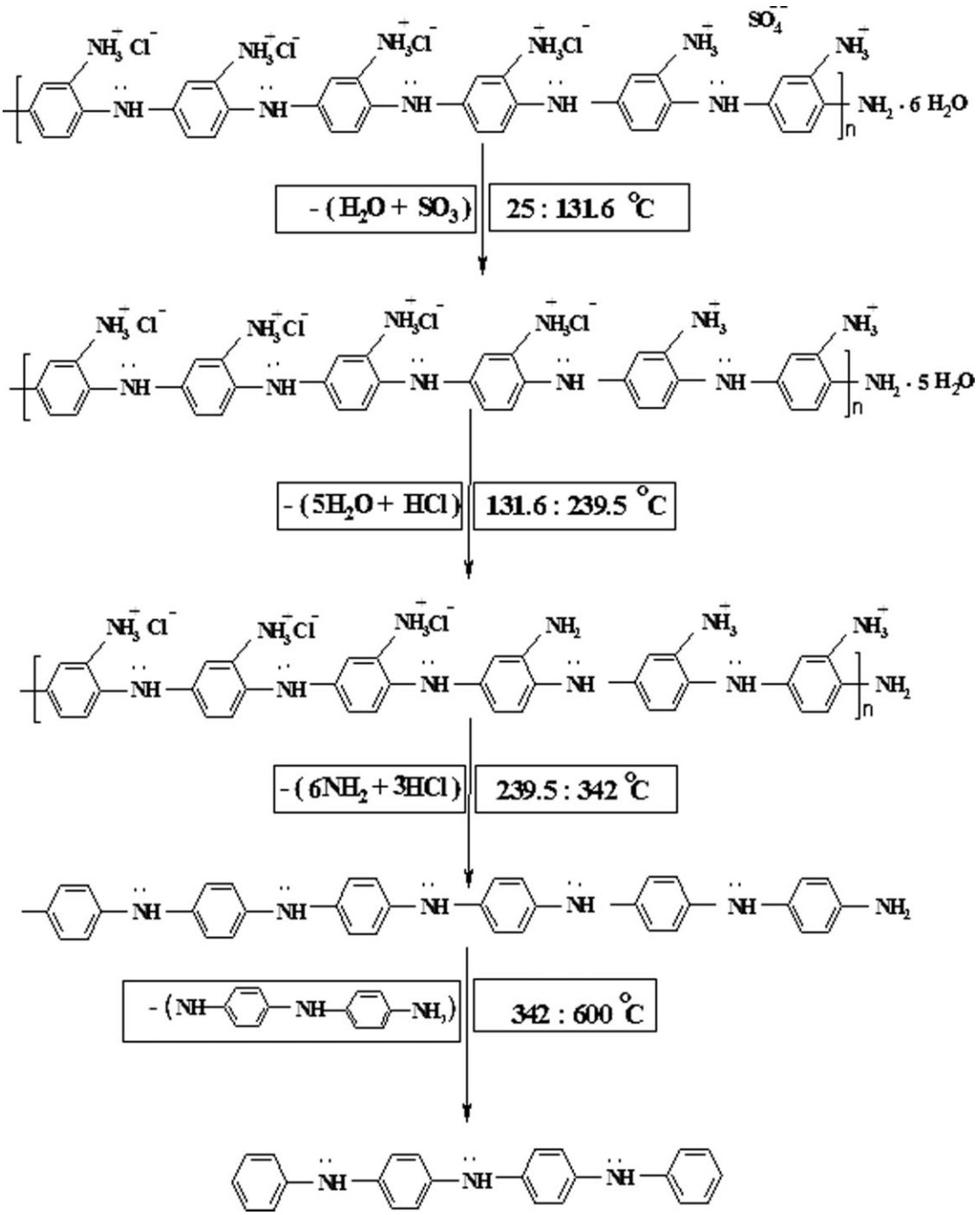

Scheme 4 Steps of thermal degradation of the prepared P(*o*-PD).

which is in good agreement with the calculated value (9.90%).

Second stage

It includes the loss of (1HCl + $5H_2O$) molecules in the temperature rang between 131.6 and 239.5°C. The weight loss for this step was found to be (12.81%) which is in good agreement with the calculated value (12.79%).

Third stage

In the temperature range between 239.5 and 342°C, the weight loss was found to be (20.01%) which is attributed to the lost of (3HCl + $6NH_2$) groups. The

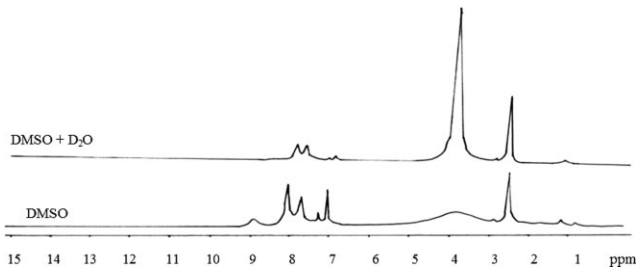

Figure 9 ^{1}H-NMR of poly(*o*-phenylenediamine) in DMSO and DMSO+D_2O.

calculated weight loss of this stage is equal to 20.78%.

Fourth stage

In the temperature range between 342 and 600°C, the weight loss was found to be (19.88%) which is attributed to the loss of (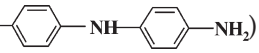) unit. The calculated weight loss of this stage is equal to 19.21%.

Fifth stage

Above 600°C, the weight loss was found to be (36.62%) which is attributed to the remaining (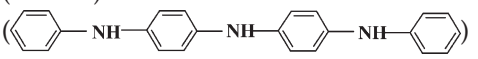) unit.

The ^{1}H-NMR spectrum of the prepared P(*o*-PD) is represented in Figure 9 The spectrum shows a two singlet signals at $\delta = 2.52$ ppm and $\delta = 3.87$ ppm which are attributed to the solvent protons. The singlet signal appears at $\delta = 7.05$ ppm could be attributed to NH protons. The doublet signals appear at $\delta = 7.2$–7.7 ppm is attributed to benzene ring protons in the polymeric structure. The singlet signals appear at $\delta = 8.04$ ppm may be attributed to NH_2 group protons. The singlet signal appears at $\delta = 8.88$ ppm is attributed to OH protons of water molecules. The signal of (OH) in different types of water molecules are disappeared when we add deuterated water to the sample.

The ^{13}C-NMR spectrum of the prepared P(*o*-PD) is represented in Figure 10 The signal at 133.588 ppm could be attributed to the carbon-bonded nitrogen (C—NH) in the benzenoid unit. The signals at (130.373, 130.273, 128.725, 127.428, 123.649, and 122.014) ppm are due to the carbon-bonded hydrogen in the benzenoid unit. The signal at 97.483 ppm may be due to carbon-bonded primary amine ($C—NH_2$) in the end group and/or noncyclized unit. The signals at 34.477 ppm and 40 ppm are attributed to the carbon-bonded hydrogen (CH_3 group of the solvent molecules). The above results confirm the suggested open structure of P(*o*-PD) (cf. Scheme 3).

The infrared absorption bands and their assignments for *o*-phenylenediamine and the prepared polymer are summarized in Table II. A medium absorption band appearing at 438.9 cm^{-1} and the weak absorption band appearing at 459.3 cm^{-1} in case of monomer appears as a weak absorption bands at 472.5 cm^{-1} in case of polymer which could be attributed to CH wagging deformation of 1,2-disubstituted benzene ring. The very weak absorption band appearing at 670 cm^{-1} in case of monomer appears at 691 cm^{-1} in case of polymer which could be attributed to NH_2 wagging deformation. A strong absorption band at 750 cm^{-1} in case of monomer appears as a medium absorption band at 726.7 cm^{-1} and a strong absorption band at 752 cm^{-1} in case of polymer which could be attributed to the CH stretching vibration of benzene ring. The weak absorption band appearing at 1130 cm^{-1} in case of polymer could be attributed to SO_4^{2-} incorporation in the polymeric chain. The strong absorption band appearing at 1057 cm^{-1} in case of monomer appears as a weak band at 1050 cm^{-1} in case of polymer which could be attributed to NH_2 twisting deformation. The weak absorption band appearing at 1169 cm^{-1} is attributed to Cl^- incorporation in case of polymer. Accordingly, both SO_4^{2-} and Cl^- anions are doped in the polymeric chain.[48,49] But no evidence for the formation of new bonds between the polymer

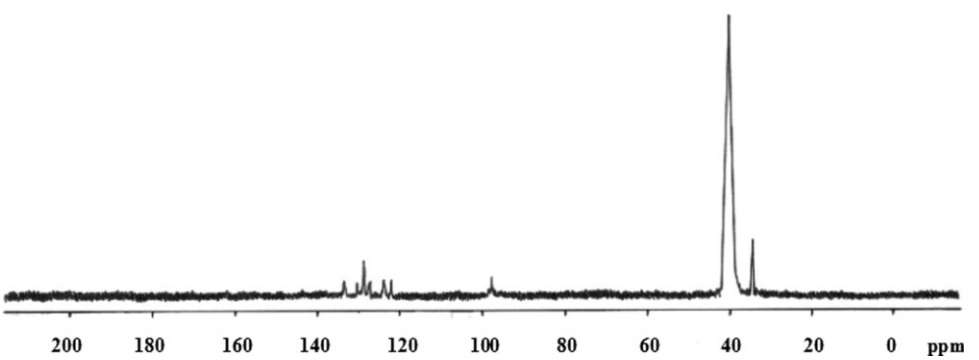

Figure 10 ^{13}C-NMR of poly(*o*-phenylenediamine) in DMSO.

TABLE II
The Infrared Absorption Bands and Their Assignments for *o*-Phenylenediamine Monomer and the Prepared Polymer

Wave number (cm^{-1})		
Name		
Monomer	Polymer	Assignments
438.9^{m}		CH wagging deformation
459.3^{w}	472.5^{w}	of 1,2-disubstituted benzene ring
539.9^{w}	510^{vw}	Out-of-plane deformation of ring
	584^{m}	
670^{vw}	691^{w}	NH_2 wagging deformation
	726.7^{m}	CH Stretching vibration of benzene ring
750^{s}	752^{s}	
799^{w}	800^{vw}	CH out-of-plane deformation
833^{w}	841.1^{w}	
927^{s}	887^{w}	
1029.2^{s}	1020^{m}	CH in-plane deformation
1057^{s}	1050^{w}	NH_2 twist deformation
1116^{m}	1120^{vw}	CH stretching vibration
1153^{m}	1145^{vw}	
1200^{w}	1205^{s}	
. . ..	1130^{w}	SO_4^{-2} incorporation
	1169^{w}	Cl^{-1} incorporation
1272^{s}	1250^{w}	C—NH_2 stretching vibration
1324^{w}		C—C stretching vibration
1400^{vw}	1365^{s}	
1458^{s}	1400^{vw}	
1500^{s}	1474^{s}	
1590^{s}	1529^{s}	
1632^{s}	1624^{s}	NH_2 scissoring vibration
	1685^{vw}	
	3008^{vw}	CH stretching vibration
3031.7^{b}	3028^{w}	
3160^{vw}	3139^{b}	NH_2 symmetric vibration
3288^{b}	3200^{b}	NH_2 asymmetric stretching
3363.3^{s}		vibration of aromatic amine
3385^{s}	3385^{b}	NH_2 asymmetric stretching vibration of aromatic amine or OH strong hydrogen bonded group in H_2O molecules of hydration in polymer.

s, strong; w, weak; b, broad; m, medium; vw, very weak.

chain and the doped anions was observed, which means that the anions doped in the polymeric chains exist in the ionic form[50] as shown in Scheme 3. A strong absorption band appearing at 1272 cm^{-1} in case of monomer, appears as a weak absorption band at 1250 cm^{-1} in case of polymer which could be attributed to C—NH_2 stretching vibration. Other infrared absorption bands and their assignments are summarized in Table II.

The UV-Visible spectra of *o*-phenylenediamine monomer and its homopolymer are represented in Figure 11. The spectra show the following absorption bands:

1. In case of monomer, three absorption bands appear at λ_{max} = 268, 274, and 306 nm, which may be attributed to π–π* transition (E_2 band) of the benzene ring and the β-band (A_{1g} to B_{2u}).
2. In case of polymer, two absorption bands appear at λ_{max} = 269 and 280 nm, which may be attributed to π–π* transition showing a red shift. Also an absorption band appears in the visible region at λ_{max} = 482 nm, which may be due to the high conjugation of the aromatic polymeric chains.

Surface morphology

In most conditions, a homogeneous, smooth, brown, and well-adhering P(*o*-PD) films were electrodeposited on platinum electrode surface. The X-ray diffraction pattern shows that the prepared polymer is

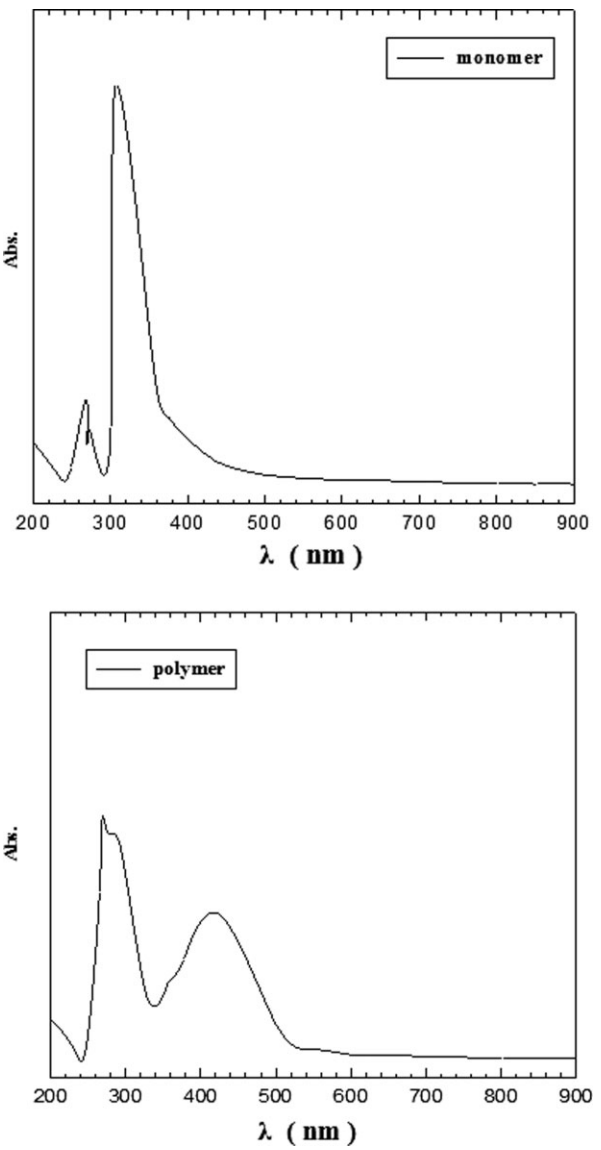

Figure 11 UV-Vis spectra of *o*-phenylenediamine monomer and the prepared polymer.

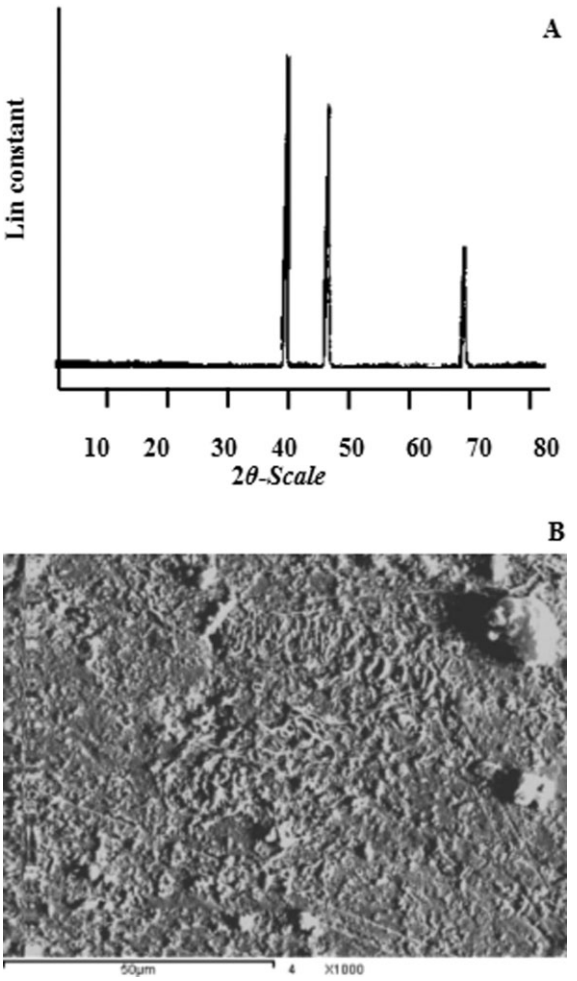

Figure 12 (A) X-ray diffraction pattern of poly(*o*-phenylenediamine). (B) The picture of scanning electron microscope of poly(*o*-phenylenediamine).

amorphous material as shown in Figure 12(A). The surface morphology of the polymer obtained at the optimum conditions was examined by scanning electron microscopy. The SEM micrograph shows a smooth surface feature with uniform thickness and has amorphous nature [cf. Fig. 12(B)].

CONCLUSIONS

In conclusion, the above data reveals the following:

1. The initial rate of electropolymerization reaction of P(*o*-PD) on platinum electrode is relatively low. The fraction of the dissolved product may be strongly dependent on temperature and monomer or HCl concentrations.
2. The orders of the electropolymerization reaction of P(*o*-PD) on platinum electrode are 1.23, 1.19, and 0.87 with respect to HCl, monomer, and electrolyte concentration, respectively.
3. The apparent activation energy is calculated to be 28.34 kJ mol^{-1}.
4. The prepared P(*o*-PD) shows a smooth surface feature with uniform thickness and has amorphous nature, and well-adhered on platinum electrode surface.
5. From cyclic voltammetry studies, it is clear that the cyclic voltammogram consists of one irreversible peak at + 609 mV versus SCE, corresponding to the conversion of amine nitrogens to radical cations.
6. The electrodeposition of the polymer film on platinum electrode may be described partially by a diffusion-controlled process.
7. The proposed mechanism, depending on the characterized tools used, is a 1,4-substituted benzenoid "open" structure one and agree with that obtained in H_2SO_4 by Yano[37] but with no quinoid units.

The authors gratefully acknowledge the assistance of Prof. Dr. S.S. Abd El-Rehim (Chemistry Department, Faculty of Science, Ain-Shams University, Cairo, Egypt) for helpful discussions and valuable supports.

References

1. Kobayashi, T.; Yoneyama, H.; Tamura, H. J Electroanal Chem 1984, 161, 419.
2. Kitani, A.; Kaya, M.; Sasaki, K. J Electrochem Soc 1986, 133, 1069.
3. MacDiarmid, A. G.; Yang, L. S.; Hung, W. S.; Humphray, B. D. Synth Met 1987, 18, 393.
4. Girard, F.; Ye, S.; Laperriere, G.; Belanger, D. J Electroanal Chem 1992, 334, 35.
5. Ye, S.; Girard, F.; Belanger, D. J Phys Chem 1993, 97, 12373.
6. Ye, S.; Belanger, D. J Electrochem Soc 1994, 141, 149.
7. Nakajima, T.; Kawagoe, T. Synth Met 1989, 28C, 629.
8. Geniès, E. G.; Lipkowski, M.; Santier, C.; Viel, E. Synth Met 1987, 18, 631.
9. Gottesfeld, S.; Redondo, A.; Feldberg, S. W. J Electrochem Soc 1987, 134, 271.
10. Nguyen, M. T.; Deo, L. H. J Electrochem Soc 1989, 136, 2131.
11. Paul, E. W.; Ricco, A. J.; Wrighton, M. S. J Phys Chem 1985, 89, 1441.
12. Chao, S.; Wrighton, M. S. J Am Chem Soc 1987, 109, 6627.
13. Dhaw, S. K.; Trivedi, D. C. Polym Int 1991, 25, 55.
14. Joseph, J.; Trivedi, D. C. J Bull Electrochem 1992, 22, 563.
15. Thanachasai, S.; Rokutanzono, S.; Yoshida, S.; Watanabe, T. Anal Sci 2002, 18, 773.
16. Garcia, M. A. V.; Blanco, B. T.; Ivaska, A. J. Electrochim Acta 1998, 43, 3533
17. Nagoaka, T.; Kakuma, K.; Fujimoto, M.; Nakao, H.; Yano, J.; Ogura, K. J Electroanal Chem 1994, 369, 315.
18. Anglopoulos, M. IBM J Res Dev 2001, 45, 57.
19. Sathiyanarayanan, S. K.; Dhawan, S.; Trivedi, D. C.; Balakrishnan, K. Corros Sci 1992, 33, 1934.
20. Sazou, D.; Georgolios, C. J Electroanal Chem 1997, 429, 81.
21. Troch-Nagels, G.; Winand, R.; Weymeersch, A.; Renard, L. J Appl Electrochem 1992, 22, 756.
22. Bernard, M. C.; Joiret, S.; Hugot-LeGoff, A.; Phong, P. V. J Electrochem Soc 2001, 148, 12.
23. Brusic, V.; Anglopoulos, M.; Graham, T. J Electrochem Soc 1997, 144, 436.

24. Su, W.; Iroch, J. O. Synth Met 1998, 95, 159.
25. Dimitra, S. Synth Met 2001, 118, 133.
26. Camalet, J. L.; Lacroix, J. C.; Aeiyach, S.; Chame-Ching, K.; Lacaze, P. C. Synth Met 1998, 93, 133.
27. Kinlen, P. G.; Ding, Y.; Silverman, D. C. Corrosion 2002, 58, 490.
28. Yagan, A.; Perkmez, N. O.; Yildiz, A. Electrochim Acta 2008, 53, 2474.
29. Wieck, H. J.; Yacynych, A. M. Anal Chem 1980, 52, 345.
30. Ohnuki, Y.; Matsuda, H.; Ohsaka, T.; Oyama, N. J Electroanal Chem 1983, 158, 55.
31. Lowry, J. P.; McAteer, K. S.; El Atrash, S.; Duff, A.; O'Neill, R. D. Anal Chem 1994, 66, 1754.
32. Centonze, D.; Malitesta, C.; Palmisano, F.; Zambonin, P. G. Electroanalysis 1994, 6, 423.
33. Chiba, K.; Ohsaka, T.; Oyama, N. J Electroanal Chem 1987, 217, 239.
34. Chiba, K.; Ohsaka, T.; Ohnuki, Y.; Oyama, N. J Electroanal Chem 1987, 219, 117.
35. Oyama, N.; Ohsaka, T.; Chiba, K.; Takahashi, K. Bull Chem Soc Jpn 1988, 61, 1095.
36. Ogura, K.; Kokura, M.; Yano, J.; Shigi, H. Electrochem Acta 1995, 40, 2707.
37. Yano, J. J Polym Sci Part A: Polym Chem 1995, 33, 435.
38. Wu, L.-L.; Luo, J.; Lin, Z.-H. Electroanal Chem 1996, 417, 53.
39. Sayyah, S. M.; El-Rabiey, M. M.; Abd El-Rehim, S. S.; Azooz, R. E. J Appl Polym Sci 2008, 109, 1643.
40. Sayyah, S. M.; Abd El-Rehim, S. S.; El-Deeb, M. M. J Appl Polym Sci 2004, 94, 941.
41. Sayyah, S. M.; Kamal, S. M.; Abd El-Rehim, S. S.; Ibrahim, M. A. Int J Polym Mater 2006, 55, 339.
42. Sayyah, S. M.; Azooz, R. E.; El-Rabiay, M. M.; Abd El-Rehim, S. S. Int J Polym Mater 2006, 55, 37.
43. Sayyah, S. M.; Kamal, S. M.; Abd El-Rehim, S. S. Int J Polym Mater 2006, 55, 79
44. Sayyah, S. M.; El-Rabiay, M. M.; Abd El-Rehim, S. S.; Azooz, R. E. J Appl Polym Sci 2006, 99, 3093.
45. Sayyah, S. M.; Kamal, S. M.; Abd El-Rehim, S. S. Int J Polym Mater Sci 2007, 56, 663.
46. Sayyah, S. M.; El-Deeb, M. M. J Appl Polym Sci 2007, 103, 4047.
47. Mu, S.; Chen, C.; Wang, J. Synth Met 1997, 88, 249.
48. Nakanishi, K.; Solomon, P. H. Infrared Absorption Spectroscopy; Holden—Day: San Francisco, 1977.
49. Athawale, A. A.; Deore, B.; Vedpathak, M.; Kulkarni, S. K. J Appl Polym Sci 1999, 74, 1286.
50. Mu, S.; Kan, J. Synth Met 1998, 98, 51.